Engineering Fracture Mechanics xxx (xxxx) xxx–xxx

Contents lists available at ScienceDirect

Engineering Fracture Mechanics

journal homepage: www.elsevier.com/locate/engfracmech

Static and dynamic mode I fracture toughness of rigid PUR foams under room and cryogenic temperatures

Emanoil Linul[a], Liviu Marşavina[a,*], Cristina Vălean[a], Radu Bănică[b]

[a] Politehnica University of Timisoara, Department of Mechanics and Strength of Materials, 1 Mihai Viteazu Avenue, 300 222 Timisoara, Romania
[b] National Institute of Research and Development for Electrochemistry and Condensed Matter, Aurel Paunescu Podeanu Street 144, 300 569 Timisoara, Romania

ARTICLE INFO

Keywords:
Closed-cell rigid polyurethane foams
Quasi-static and dynamic 3PB tests
Mode I fracture toughness
Room and cryogenic temperatures
Anisotropy

ABSTRACT

The research presented in this paper is an effort to better understand the fracture toughness of closed-cell rigid polyurethane (PUR) foams under different loading and temperature conditions. The effect of density (100, 145 and 300 kg/m^3) and anisotropy (in-plane and out-of-plane loading directions) on both quasi-static and dynamic fracture behavior was also experimentally investigated. The three-point bending (3PB) tests were performed on Single Edge Notched Bend (SENB) samples, at room (25 °C) and cryogenic (−196 °C) temperatures, and the mode I fracture toughness (K_{IC}) was calculated from their load-displacement curves. It was observed that all PUR foam samples, regardless of foam density and loading direction, showed a significant increase in K_{IC} at the cryogenic temperature. The out-of-plane obtained samples showed a slight improvement in fracture toughness (highlighting an anisotropic behavior), both under quasi-static and dynamic 3PB loads. The dynamic K_{IC} values were found higher than quasi-static ones, and irrespective of foam density and test condition, a brittle deformation mechanism without plastic deformation was observed for all samples. Finally, empirical formulations for cryogenic and dynamic K_{IC} based on room temperature mode I fracture toughness were proposed.

1. Introduction

Porous materials such as metallic [1–3] and polymeric [4–6] closed-cell foams are being increasingly used in many structural and functional engineering applications, because of their high crashworthiness performances, lightweight, high porosity and good energy absorption capacity [7–9]. Due to their closed-cellular structure and unique properties, porous materials have found new applications in the automotive and aerospace industries, and are preferred to fully dense solid materials [10–12]. Closed-cell rigid PUR foam materials are widely used as cores in sandwich composites, for packing and cushioning [13,14].

Many experimental efforts have been made in recent years to determine the mechanical properties of foam materials through compression [15–17], tensile [18–20], bending [21–23], shear [24,25], fracture toughness [4,26,27] and fatigue [28–30] tests. Foams progressively crush in compression to a relatively high strain under an approximately constant load, while in tension fail by propagating of single crack [31–33]. Most of the rigid polymeric foams have a linear-elastic behavior in tension up to fracture and a brittle failure behavior. Therefore, rigid PUR foams can be treated using Linear Elastic Fracture Mechanics criteria.

Different teams of researchers presented different aspects of the fracture and failure assessment of PUR foam materials, like analytical micromechanical models, numerical simulations and experimental determination of fracture toughness [34–37]. However,

* Corresponding author.
E-mail address: liviu.marsavina@upt.ro (L. Marşavina).

https://doi.org/10.1016/j.engfracmech.2018.12.007
Received 28 August 2018; Received in revised form 13 November 2018; Accepted 6 December 2018

Nomenclature

a	crack length of the sample
B	width of the sample
CT	cryogenic temperature
F	applied load
Fs	fractured surface
Fs-Ns	fractured-notch interface
f(a/w)	dimensionless SIFs shape function for SENB sample
K_I	mode I stress intensity factor
K_{IC}	mode I fracture toughness
$K_{IC,D}$	dynamic mode I fracture toughness
$K_{IC,QS}$	quasi-static mode I fracture toughness
$K_{IC,25}$	quasi-static mode I fracture toughness at 25 °C
$K_{IC,-196}$	quasi-static mode I fracture toughness at −196 °C
l	cell length
LD	loading direction
LN	liquid nitrogen
Ns	notch surface
P	porosity
F_Q	fracture load
PUR	polyurethane
QS	quasi-static test
RT	room temperature
SEM	scanning electron microscope
SENB	single edge notched bend
SIF	stress intensity factor
t	cell-wall thickness
UTS	ultimate tensile strength
W	height of the sample
3PB	three point bending
Δ	displacement
ρ^*	density of rigid PUR foam
ρ_s	density of solid material
ρ^*/ρ_s	foam relative density
σ_{max}	maximum tensile strength

most of these studies have been focused on quasi-static loads and under room temperature testing conditions. The main physico-mechanical cryogenic properties (thermal conductivity, thermal expansion, modulus in compression/tension/bending, elongation - elastic and plastic -, yield strength, tensile/shear/compressive strengths, etc.) of different polymeric foams, the effects of low temperature on fracture toughness and fatigue debond growth rate of foam core sandwich composites, were extensively investigated [38–40]. Yakushin and co-workers [41] studied the effect of basic processing factors on the inhomogeneity of the structure and physico-mechanical characteristics of spray-on rigid foam polyurethane at 20 °C and −182 °C. They determined the properties of the foam both in the core of sprayed-on plates and in the surface skin. Studies on the effect of the foams' polymeric matrix' properties on the tension and compression properties (Young's modulus, tensile strength and elongation at break) of PUR foams at 23 and −196 °C were carried out by Stirna et al. [42]. In the study of Denay et al. [43] the effects of negative temperatures (between 0 and −170 °C) on compression behavior of non-reinforced and glass-fiber-reinforced PUR foams is presented. A non-linear increase of modulus and yield stress was observed with decreasing temperature. Yakushin et al. [44] investigated the effect of filler type and mass percentage on the properties of low-density rigid polyurethane foams at a temperature of −196 °C. A considerable increase in the compressive elastic modulus in the foam rise direction with increasing filler content was observed.

To the author's knowledge, no study on fracture toughness determination of rigid PUR foams at cryogenic temperature has been published to date. Aspects such as low operating temperatures and related failure mechanisms of PUR foams are yet unfamiliar. Therefore, the aim of the present work is to determine the mode I fracture toughness values of different closed-cell rigid polyurethane foams at room (25 °C) and cryogenic temperature (−196 °C) under both quasi-static and dynamic loading conditions. Furthermore, the foam anisotropy (in-plane and out-of-plane loading directions) together with foam microstructure (before and after 3PB tests) are assessed according to operating temperatures.

2. Experimental details

2.1. Materials and sample preparation

All samples were obtained by cutting them from three different large panels of rigid polyurethane foam (named Necuron 100,

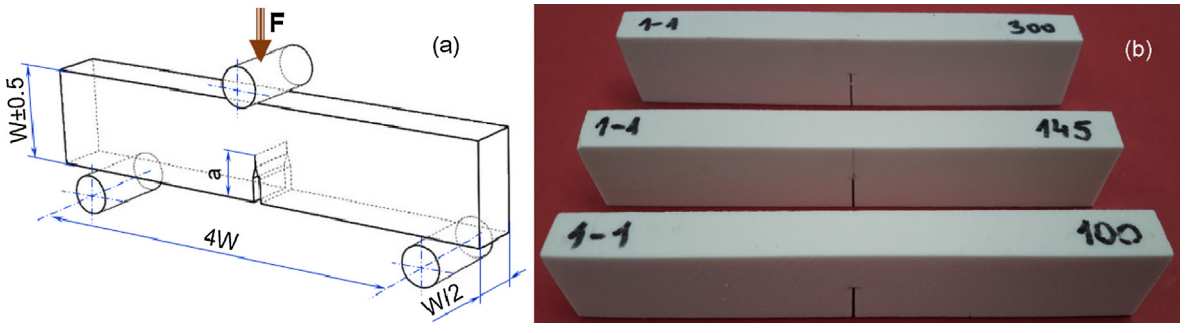

Fig. 1. Geometrical parameters (a) and obtained (b) SENB samples used for 3PB tests.

Necuron 160 and Necuron 301), produced by Necumer GmbH, Germany. Each foam panel has a different density and its determination together with the geometric parameters of the foam microstructure will be presented in detail in Section 3.1.

Single Edge Notch Bend (SENB) samples were adopted for both Quasi-Static (QS) and dynamic three Point Bending (3PB) tests with width W = 25 mm, thickness B = W/2 = 12.5 mm, and span length S = 4 W = 100 mm. At least four samples were tested for each density and each loading direction. The crack has been produced artificially by using a razor blade (0.6 mm thickness) and cutting the foam to the desired initial crack length of a = 12.5 mm. Fig. 1a present the geometrical parameters of the investigated samples, while Fig. 1b show the manufactured foam samples before testing with different densities.

The mode I fracture toughness of anisotropic closed-cell polyurethane foams depends on the direction in which the crack initiates and propagates [6]. Therefore, the SENB samples were cut after two main directions (see Fig. 2), associated at the same time with both the foam formation and loading directions: *foam rise direction* (direction (1) or out-of-plane loading direction), and *foam flow direction* (direction (2) or in-plane loading direction).

2.2. Experimental test set-up

Quasi-Static 3PB tests were carried out on a 5 kN Zwick Roell 005 testing machine with a constant crosshead speed of 2 mm/min, according to D5045-99 standard [45]. The QS 3PB tests were performed under two different temperatures as follows: 25 °C (room temperature or RT) and −196 °C (cryogenic temperature or CT). Fig. 3 shows photographs of the experimental setup for the cryogenic fracture toughness tests. All 3PB samples were precooled at −196 °C in the cryogenic test stand for 10 min. In order to prevent any reduction in temperature after precooling, the 3PB samples were tested inside the cryogenic stand test. Practically, the low temperature 3PB sample tests are performed submerged in liquid nitrogen (LN).

A KB Pruftechnik pendulum (Germany) was used for the instrumented impact (dynamic) tests, according to EN ISO 179-2-*2000* [46] and Katthoff [47]. The main characteristics of used pendulum are presented in detail in Ref. [48].

The load-displacement curves were recorded and the load F_Q for calculation of fracture toughness was determined in accordance with [45]. The fracture toughness (K_{IC}) was calculated according to [45] based on Eq. (1), using the geometrical parameters of the samples.

$$K_{IC} = \frac{F_Q}{BW^{0.5}} f\left(\frac{a}{W}\right) [\mathrm{MPa \cdot m^{0.5}}] \tag{1}$$

were F_Q is the critical fracture load in [N], B and W are sample dimensions in [mm], a is the crack length in [mm], while f(a/W) is a geometric factor expressed in terms of a/W by Eq. (2) [45]:

$$f\left(\frac{a}{W}\right) = 6\sqrt{\frac{a}{W}} \frac{1.99 - (a/W)(1 - a/W)[2.15 - 3.93(a/W) + 2.7(a/W)^2]}{(1 + 2a/W)(1 - a/W)^{1.5}} \tag{2}$$

3. Experimental results

3.1. Physical properties of closed-cell rigid PUR samples

Fig. 3 shows the microstructure morphology of the investigated closed-cell PUR foams. Due to the large/small dimensions and random scattering of the cells, the density of the foam samples varies in certain intervals. The average densities together with geometrical parameters of the cells (cell length and cell-wall thickness) are presented in Table 1. The samples with density above or below the 5% range were excluded prior experiments.

The samples density of the investigated PUR foams was calculated by dividing the mass of each sample by its volume, according to

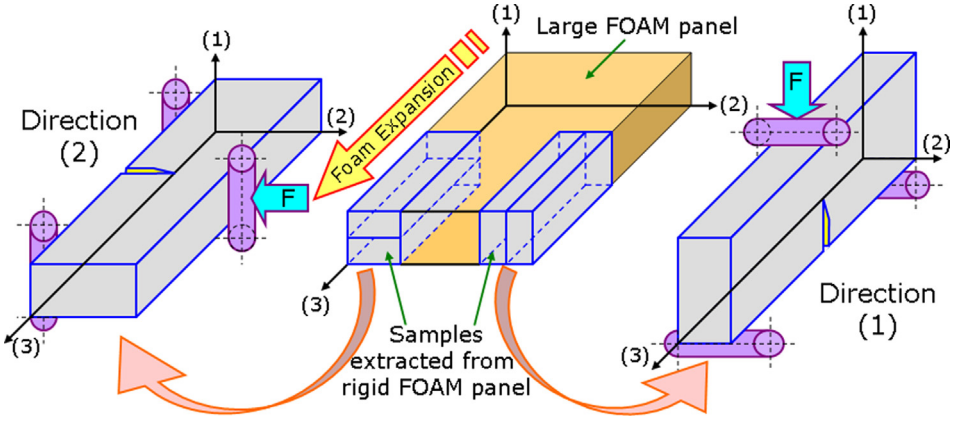

Fig. 2. The cutting directions of SENB samples from a large PUR foam panel.

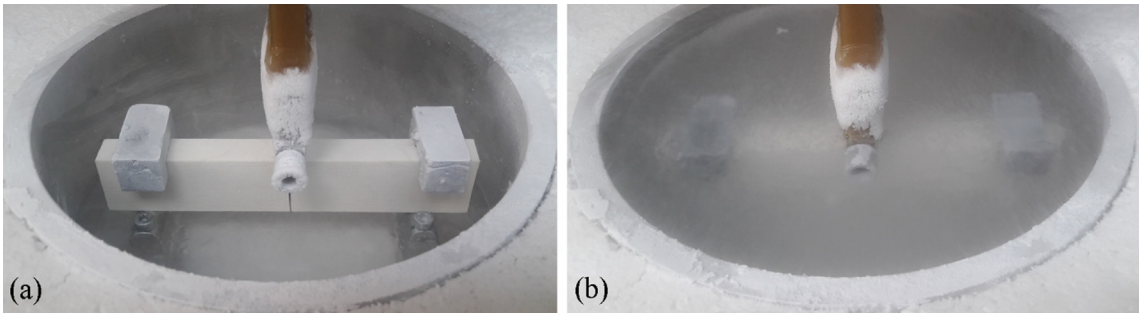

Fig. 3. Experimental setup for the cryogenic experiment: photographs of the test stand before (a) and after immersing (b) the sample in LN.

Table 1
Density, porosity and geometrical parameters of the foam structures [49].

Foam type	Necuron 100	Necuron 160	Necuron 301
Density, ρ [kg/m^3]	100.37 ± 0.25	145.53 ± 0.22	300.28 ± 1.38
Porosity, P [%]	91.42 ± 0.02	87.56 ± 0.02	74.33 ± 0.12
Cell length in-plane, l [μm]	104.50 ± 9.40	83.80 ± 9.60	68.50 ± 33.90
Cell length out-of-plane, l [μm]	120.20 ± 14.50	88.10 ± 11.20	67.80 ± 32.10
Cell-wall thickness, t [μm]	4.35 ± 1.45	9.10 ± 3.99	12.80 ± 8.99

ASTM D 1622-03 standard [50]. The porosity of foam samples was calculated by Eq. (3) [51]:

$$P = 1 - \frac{\rho^*}{\rho_s} \tag{3}$$

where P is the porosity percent, ρ^* is the density of foam and ρ_s is the density of the solid material from which foam has been produced. As it can be seen from the microstructure of the produced PUR foams (see Fig. 4), the porosity distribution is almost homogenous throughout the selected samples with morphologies ranged from spherical to ellipsoid shapes.

An examination of the microstructure (Fig. 4) indicates that the foams have a typical closed-cell structure [52]. From both Table 1 and Fig. 4, it is seen that the low-density foams (100 and 145 kg/m^3) exhibit a wide variation in pore size and shape, while the high-density foam (300 kg/m^3) exhibit smaller uniform sized pores separated by large amount of solid polymer. Both the SEM images obtained for direction (1) and direction (2) show approximately the same shape of the cells for each density. The measurement of the geometrical parameters of foams pores was carried out with Sigma Scan Pro software.

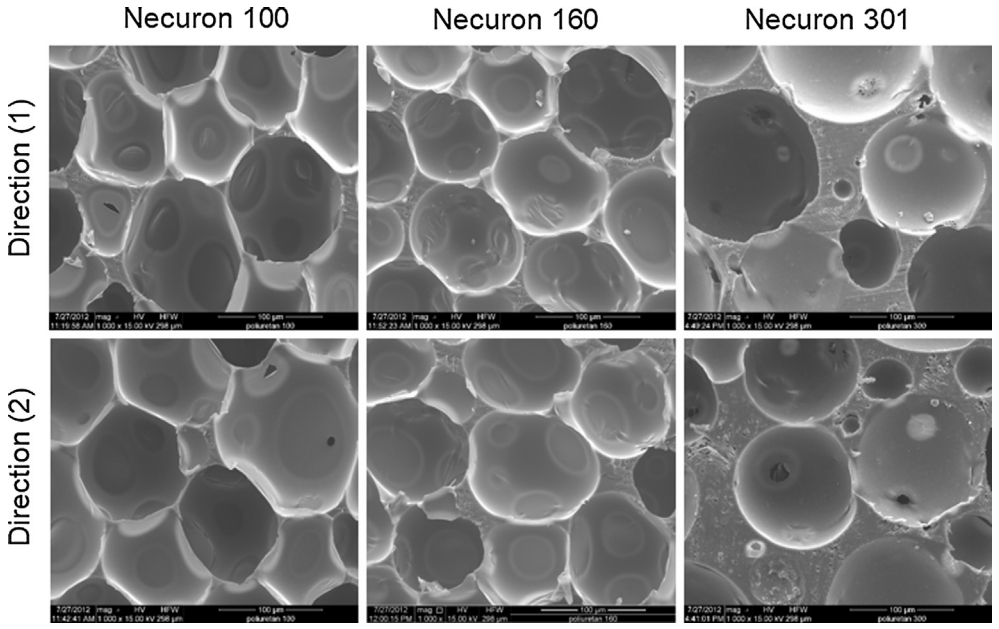

Fig. 4. SEM images of rigid PUR foams before testing (magnification 1000×).

3.2. Quasi-static mode I fracture toughness of PUR samples

The load (F) - displacement (Δ) data was recorded by an built-in data acquisition software incorporated in the test machine. In this case, Δ is the displacement of the point of application of load. Fig. 4 presents the F - Δ curves obtained under quasi-static 3PB tests on notched samples for both out-of-plane (full lines) and in-plane (dashed lines) loading directions. The graphs are obtained at RT (Fig. 5a) and CT (Fig. 5b) for three different densities. The F - Δ curves show a linear-elastic behavior with quasi-brittle failure, more brittle failure being observed at −196 °C.

The mechanism that make the displacement of out-plane in CT large than in-plane for 100 and 145 kg/m^3 foams densities (while in RT the law is opposite), is probably due to the small cell-wall thickness of low density foams. It seems that for lower densities, the deformation mechanism is more unstable than for high density.

Due to brittle behavior of rigid PUR foams under RT and CT, the maximum load from load-displacement curves was used in the calculation of fracture toughness. Therefore, Table 2 shows the main mode I quasi-static fracture toughness values (together with standard deviations) of investigated foams for in-plane and out-of-plane loading directions.

The critical fracture load (F_Q) from Fig. 5, corresponding to each foam density is significantly higher for the experimental tests performed at −196 °C than 25 °C. This aspect can be seen much easily in the calculated mode I fracture toughness values from Table 2. Also, F_Q increases with the increase in foam density. However, the displacement at break decreased for both investigated loading directions, and it was especially significant on the in-plane loading direction. The Δ reduction from RT to CT can be addressed to the dominant mechanical behavior of the solid material from which the foam is made.

The geometrical parameters of the used tensile samples together with the ultimate tensile strength (UTS) data and the plain strain condition are presented in Table 3. As it can be seen from Table 3, the quasi-static room temperature K_{IC} results fulfill the plane strain condition according with standard (D5045) requirements [45].

Testing of cellular materials in traction is very difficult even at RT, because the clamping of the samples destroys the foam cells. Performing static tensile tests at CT or even dynamic tensile tests was not possible. In addition, the literature review does not show UTS values for the investigated foams and densities. Therefore, the plain strain values for cryogenic and dynamic values are not available. However, extrapolating the values obtained for static RT tests, the authors consider (at least until cryogenic and dynamic tensile tests are possible) that these values can be met also the dynamic/cryogenic plane strain condition.

3.3. Dynamic mode I fracture toughness of PUR samples

Fig. 6 presents the load-displacement curves obtained for the investigated rigid PUR foams, during dynamic tests at 25 °C, while Table 4 shows the calculated dynamic mode I fracture toughness ($K_{IC,D}$) values. The $K_{IC,D}$ was determined following the same procedure as in the case of QS tests.

Like in the static tests, the maximum load for the dynamic F-Δ curves increases with the increase in foam density. Also, there are considerable differences between the 3PB tests performed in-plane and out-of-plane loading direction.

3.4. Microstructural analysis of fractured PUR foam samples

Fig. 7 presents the obtained SEM images of the investigated PUR foam cracked samples after quasi-static 3PB tests at cryogenic temperature. The images are presented for fractured surfaces (Fs), notched surfaces (Ns) and Fs-Ns interfaces of tested samples. After mode I loading, brittle fracture for all tested PUR foam samples was observed, regardless of foam density and loading direction. The linear-elastic behavior of load-displacement curves (Fig. 5a) was confirmed during the 3PB tests when no cushioning occurs and there remained no plastic deformation of the cell-walls after the cryogenic temperature tests (Fig. 7).

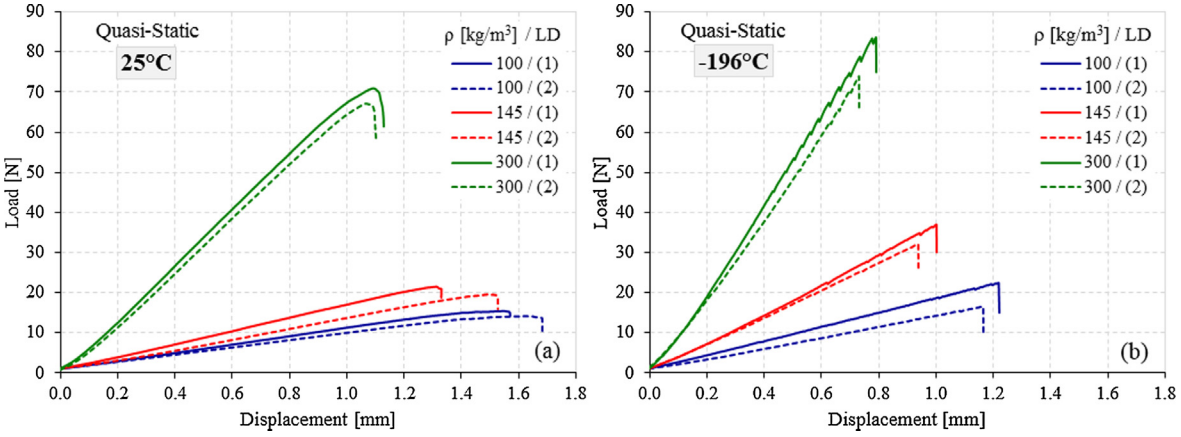

Fig. 5. QS load-displacement curves at 25 °C (a) and −196 °C (b) for different foams densities.

Table 2
Quasi-static mode I fracture toughness values of PUR foams at RT and CT.

Testing temperature [°C]	Density [kg/m^3]	Fracture toughness [MPa·m$^{0.5}$]	
		Out-of-plane	In-plane
25	100	0.076 ± 0.006	0.072 ± 0.003
25	145	0.116 ± 0.010	0.109 ± 0.012
25	300	0.355 ± 0.028	0.331 ± 0.009
−196	100	0.110 ± 0.008	0.092 ± 0.007
−196	145	0.187 ± 0.006	0.178 ± 0.008
−196	300	0.417 ± 0.015	0.393 ± 0.012

Table 3
The geometrical parameters of tensile samples, UTS data and the plain strain condition.

Foam density	Loading direction	Geometrical parameters			Yield stress	Plain strain condition $2.5(K_Q/\sigma_{max})^2$		
		Crack length, a	Sample width, B	W-a	σ_{max}	Static tests		Dynamic tests
[kg/m^3]		[mm]	[mm]	[mm]	[MPa]	25 °C	−196 °C	25 °C
100	out-of-plane	12.5	12.5	12.5	1.22	8.77 ± 0.61	NA	NA
	in-plane	12.5	12.5	12.5	1.28	8.92 ± 0.85		
145	out-of-plane	12.5	12.5	12.5	1.97	6.86 ± 0.45		
	in-plane	12.5	12.5	12.5	2.11	6.84 ± 0.13		
300	out-of-plane	12.5	12.5	12.5	4.38	11.48 ± 0.37		
	in-plane	12.5	12.5	12.5	4.69	11.98 ± 0.22		

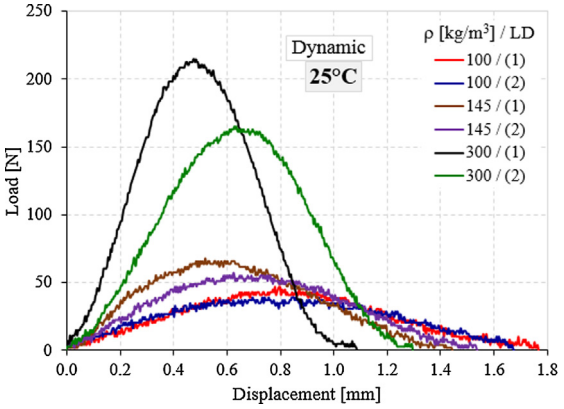

Fig. 6. Dynamic load-displacement curves at 25 °C for different foams densities.

Table 4
Dynamic mode I fracture toughness values of PUR foams at 25 °C.

Testing temperature [°C]	Density [kg/m^3]	Fracture toughness [MPa·m$^{0.5}$]	
		out-of-plane	in-plane
25	100	0.201 ± 0.015	0.190 ± 0.005
25	145	0.341 ± 0.016	0.293 ± 0.009
25	300	0.997 ± 0.045	0.819 ± 0.021

4. Discussions and comparative analysis

The quasi-static mode I fracture toughness values versus foam density for the in-plane and out-of-plane loading directions are presented in Fig. 8, according to operating temperature (room and cryogenic temperature). Error bars represent the scatter of experimental data; the range between the lower and higher obtained K_{IC} values. Scatter in the fracture toughness values was less than 8% regardless of density, testing temperature and loading direction, except for foam having a density of 100 kg/m^3 where 14% was

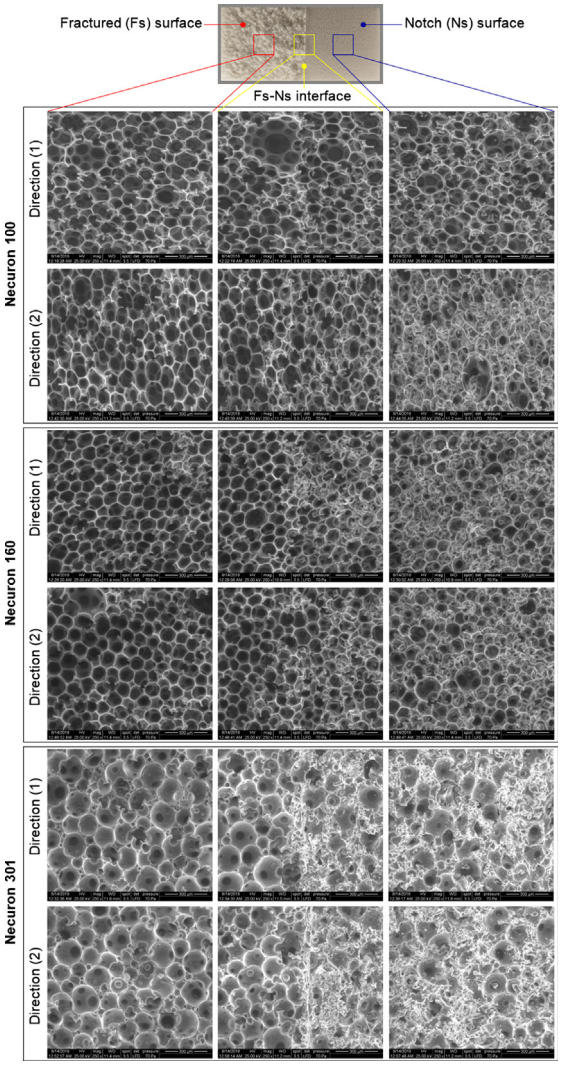

Fig. 7. SEM images of initial notch surface and fractured surface after test (magnification 250×).

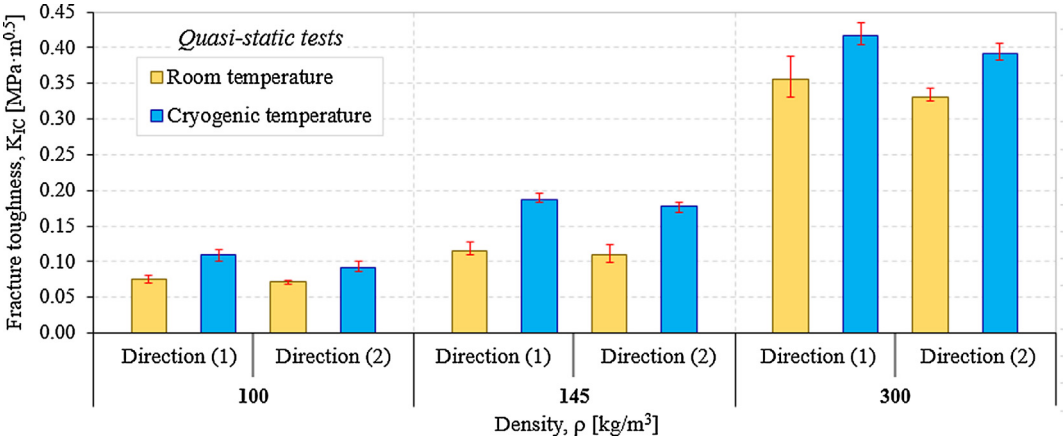

Fig. 8. Quasi-static fracture toughness results according to operating temperature.

obtained.

It is noticed that density has a significant influence on fracture toughness values, which increases with density increasing (with about 79% within the range of investigated foam densities for RT and CT). The RT out-of-plane fracture toughness values were found higher than the in-plane values with about 6% for all densities. This percentage difference increasing by up to 16% for the tests performed at −196 °C, especially for low densities (100 kg/m^3); while for high densities (300 kg/m^3) the K_{IC} difference is below 6%. Therefore, the investigated rigid PUR foams highlight an anisotropic behavior in terms of mode I fracture toughness for both room and cryogenic temperature. The anisotropy of investigated PUR foams is directly related to the geometric parameters of the cell microstructure (cells orientation, in-plane and out-of-plane cell length, in-plane and out-of-plane cell-wall thickness) [24]. On the other hand, contrary to the results reported by Yu and co-workers [53], Fig. 8 shows that the in-plane and out-of-plane CT fracture toughness values are higher than those obtained at RT, i.e. 30–39% for 100 and 145 kg/m^3, and about 15% for 300 kg/m^3. This K_{IC} difference can be explained by the influence of several factors such as testing parameters (cooling systems of the samples, test temperature, test type, etc.) and foam type (density, microstructure, shape of the cells, cell length, cell-wall thickness, etc.).

As a polymer (solid of which the foam is made) cools down, the motion and vibration of its molecules becomes more restricted, which increase the stiffness of the material, as can be observed in DMA tests from Ref. [54]. In general, two mechanisms are responsible for the fracture of polymers/polymeric foams: bond breakage and chain slippage [55]. The first mechanism is determined by the physical and chemical characteristics of the material, while the second mechanism is influenced by the viscoelastic flow of macromolecules. Even though the chain scission consumes a significant amount of the energy required to fracture a specimen, the viscoelastic effects are also important through the energy dissipated by chain slippage, especially in the beginning stages of deformation prior to fracture [56]. Therefore, considering the effect of viscoelastic flow in the fracture of polymer, and the fact that viscous flow energy increases with the decrease in temperature, it can be concluded that, in general, lower testing temperatures should determine higher fracture energies.

Fig. 9 presents the quasi-static and dynamic fracture toughness results at room temperature for in-plane and out-of-plane loading directions. Dynamic tests show a more pronounced character of anisotropy than static tests. In this case, only the density of 100 kg/m^3 shows a difference of 6% between the two loading directions (like quasi-static tests), whereas for other densities this difference reaches up to 15% for 145 kg/m^3 and 18% for 300 kg/m^3. Regardless of foam density, the dynamic K_{IC} results are up to 66% higher than the quasi-static ones for direction (1) and 62% for direction (2).

The RT dynamic mode I fracture toughness ($K_{IC,D}$) has a high importance in selecting closed-cell rigid PUR foams and composites with foam core, especially for impact applications. Quasi-static mode I fracture toughness at −196 °C ($K_{IC,-196}$) finds its relevance in advanced foamed composites from aerospace applications, where extreme temperature conditions are encountered [57]. Taking into account all these industrial requirements, Fig. 10a present a correlation between RT mode I fracture toughness ($K_{IC,25}$) and $K_{IC,-196}$, while Fig. 10b show a correlation between QS mode I fracture toughness at 25 °C ($K_{IC,QS}$) and $K_{IC,D}$.

Based on the obtained experimental data, two linear correlation equations were proposed for estimation of both $K_{IC,-196}$ and $K_{IC,D}$. The proposed correlation relations are very useful for mentioned applications because the 3PB experimental tests under cryogenic and dynamic conditions are carried out more difficult than RT QS tests. In this respect, through these simple empirical formulations both $K_{IC,-196}$ and $K_{IC,D}$ values can be estimated according to the RT quasi-static values which are obtained relatively easily Of course, the proposed correlations are valid in the investigated foam density range of 100–300 kg/m^3.

5. Conclusions

This paper investigate the effect of density (100, 145 and 300 kg/m^3), anisotropy (in-plane and out-of-plane loading directions) and testing temperature (25 °C and −196 °C) on quasi-static and dynamic mode I fracture toughness of closed-cell rigid polyurethane foams. Experimental tests were performed on SENB samples. The following conclusions can be drawn:

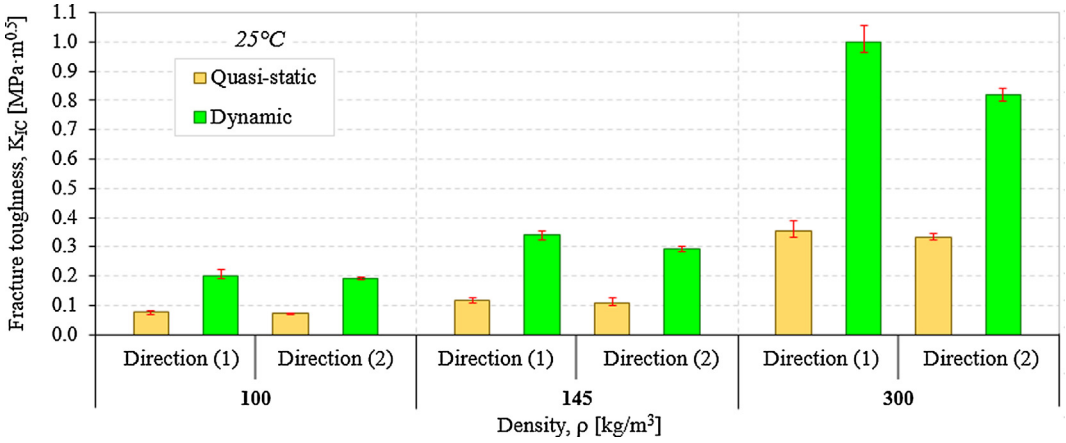

Fig. 9. Quasi-static and dynamic fracture toughness results at room temperature.

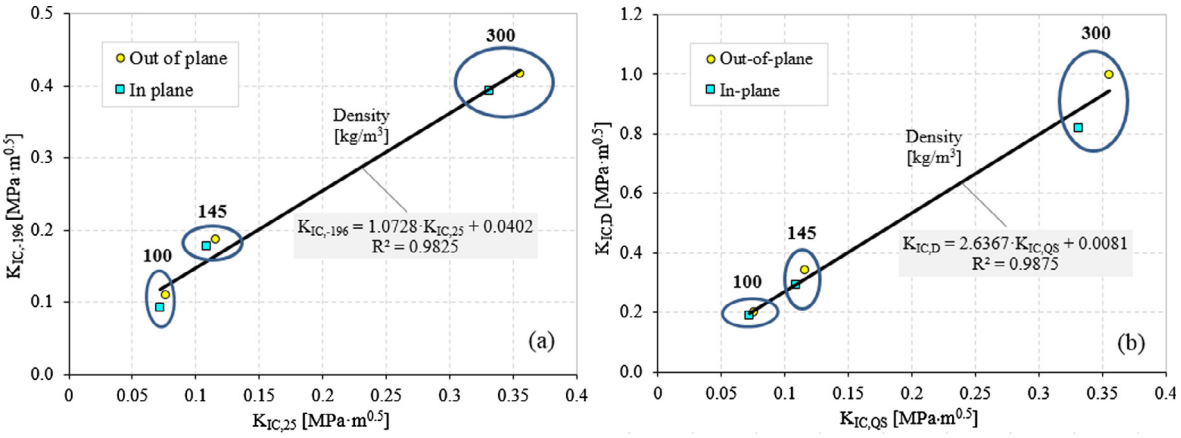

Fig. 10. Correlation between RT and CT quasi-static K_{IC} (a) and between static and dynamic K_{IC} at RT (b).

- It was found that with increasing of foam density a significant increase of mode I fracture toughness was obtained.
- The out-of-plane fracture toughness values were found higher than in-plane ones. Therefore, the investigated PUR foams exhibit an anisotropic behavior.
- Fracture toughness at CT presents higher values compared to RT. Also, the failure mechanisms is more brittle at −196 °C than at 25 °C.
- The dynamic fracture toughness values were found up to 3 times higher than quasi-static ones, especially for out-of-plane loading direction.
- The microstructural analysis confirmed (obtained from load-displacement graphs) the brittle deformation mechanism of samples without plastic deformation.
- Two empirical linear correlations for estimation of $K_{IC,-196}$ and $K_{IC,D}$ according to the RT quasi-static mode I fracture toughness values were proposed.

Acknowledgment

This work was partially supported by research grants PCD-TC-2017 fouded by Politehnica University of Timisoara, Romania and project of the Romanian Ministry of Research and Innovation, CCCDI – UEFISCDI, project number PN-III-P1-1.2-PCCDI-2017-0391 / CIA_CLIM - *Smart buildings adaptable to the climate change effects*, within PNCDI III". The authors are grateful to acknowledge colleague Radu Gurgu from Politehnica University of Timisoara (Romania) for technical assistance in building the experimental set-up.

Appendix A. Supplementary material

Supplementary data to this article can be found online at https://doi.org/10.1016/j.engfracmech.2018.12.007.

References

[1] Kovácik J, Jerz J, Mináriková N, et al. Scaling of compression strength in disordered solids: metallic foams. Frattura ed Integrita Strutturale 2016;36:55–62.
[2] Linul E, Marsavina L, Kováčik J. Collapse mechanisms of metal foam matrix composites under static and dynamic loading conditions. Mat Sci Eng A 2017;690:214–24.
[3] Ashby MF, Evans A, Fleck NA, et al. Metal foams: a design guide. USA: Butterworth-Heinemann; 2000.
[4] Marsavina L, Berto F, Negru R, et al. An engineering approach to predict mixed mode fracture of PUR foams based on ASED and micromechanical modeling. Theor Appl Fract Mech 2017;91:148–54.
[5] Linul E, Marsavina L, Sadowski T, Kneć M. Size effect on fracture toughness of rigid polyurethane foams. Solid State Phenom 2012;188:205–10.
[6] Gibson LJ. Ashby MF Cellular Solids-Structures and properties-Second edition. UK: Press Syndicate of the University of Cambridge; 1997.
[7] Linul E, Serban DA, Voiconi T, et al. Energy-absorption and efficiency diagrams of rigid PUR foams. Key Eng Mater 2014;601:246–9.
[8] Movahedi N, Linul E. Quasi-static compressive behavior of the ex-situ aluminum-alloy foam-filled tubes under elevated temperature conditions. Mater Lett 2017;206:182–4.
[9] Avalle M, Belingardi G, Montanini R. Characterization of polymeric structural foams under compressive impact loading by means of energy-absorption. Int J Impact Eng 2001;25:455–72.
[10] Şerban DA, Linul E, Voiconi T, et al. Numerical evaluation of two-dimensional micromechanical structures of anisotropic cellular materials: case study for polyurethane rigid foams. Iran Polym J 2015;24:515–29.
[11] Linul E, Marsavina L. Prediction of fracture toughness for open cell polyurethane foams by finite element micromechanical analysis. Iran Polym J 2011;20(9):736–46.
[12] Kramberger J, Šori M, Šraml M, Glodež S. Multiaxial low-cycle fatigue modelling of lotus-type porous structures. Eng Fract Mech 2017;174:215–26.
[13] Birsan M, Sadowski T, Marsavina L, et al. Mechanical behavior of sandwich composite beams made of foams and functionally graded materials. Int J Solids Struct 2013;50:519–30.
[14] Şerban DA, Voiconi T, Linul E, et al. Viscoelastic properties of PUR foams: Impact excitation and dynamic mechanical analysis. Materiale Plastice 2015;52(4):537–41.
[15] Linul E, Şerban DA, Marsavina L, Sadowski T. Assessment of collapse diagrams of rigid polyurethane foams under dynamic loading conditions. Arch Civ Mech

Eng 2017;17(3):457–66.
[16] Linul E, Movahedi N, Marsavina L. The temperature effect on the quasi-static compressive behavior of ex-situ aluminum foam-filled tubes. Compos Struct 2017;180:709–22.
[17] Mills NJ. Polymer foams handbook. Butterworth-Heinemann; 2007.
[18] Negru R, Marsavina L, Voiconi T, et al. Application of TCD for brittle fracture of notched PUR materials. Theor Appl Fract Mech 2015;80:87–95.
[19] Voiconi T, Negru R, Linul E, et al. The notch effect on fracture of polyurethane materials. Frattura ed Integrita Strutturale 2014;30:101–8.
[20] Kabir ME, Saha MC, Jeelani S. Tensile and fracture behavior of polymer foams. Mat Sci Eng A 2006;429:225–35.
[21] Linul E, Marsavina L. Assesment of sandwich beams with rigid polyurethane foam core using failure-mode maps. P. Romanian Acad A 2015;16(4):522–30.
[22] Voiconi T, Linul E, Marsavina L, et al. Determination of flexural properties of rigid PUR foams using digital image correlation. Solid State Phenom 2014;216:116–21.
[23] Thompson MS, McCarthy ID, Lidgren L, Ryd L. Compressive and shear properties of commercially available polyurethane foams. J Biomech Eng 2003;125(5):732–4.
[24] Marsavina L, Constantinescu DM, Linul E, et al. Shear and mode II fracture of PUR foams. Eng Fail Anal 2015;58:465–76.
[25] Abrate S. Criteria for yielding or failure of cellular materials. J Sandw Struct Mater 2008;10:5–51.
[26] Aliha MRM, Linul E, Bahmani A, Marsavina L. Experimental and theoretical fracture toughness investigation of PUR foams under mixed mode I+III loading. Polym Test 2018;67:75–83.
[27] Viana GM, Carlsson LA. Mechanical properties and fracture characterisation of cross-linked PVC foams. J Sandw Struct Mater 2002;4:99–113.
[28] Noble FW, Lilley J. Fatigue crack growth in polyurethane foam. J Mater Sci 1981;16(7):1801–8.
[29] Linul E, Şerban DA, Marsavina L, Kovacik J. Low-cycle fatigue behaviour of ductile closed-cell aluminium alloy foams. Fatig Fract Eng Mater Struct 2017;40(4):597–604.
[30] Lisiecki J, Nowakowski D, Reymer P. Fatigue properties of polyurethane foams, with special emphasis on auxetic foams, used for helicopter pilot seat cushion inserts. Fatig Aircraft Struct 2014;1:72–8.
[31] Linul E, Marsavina L, Kovacik J, Sadowski T. Dynamic and quasi-static compression tests of closed-cell aluminium alloy foams. P Romanian Acad A 2017;18(4):361–9.
[32] Marsavina L, Linul E, Voiconi T, et al. On the crack path under mixed mode loading on PUR foams. Frattura ed Integrita Strutturale 2015;34:444–53.
[33] Marsavina L, Constantinescu DM, Linul E, et al. Experimental and numerical crack paths in PUR foams. Eng Fract Mech 2016;167:68–83.
[34] Linul E, Serban DA, Marsavina L. Influence of cell topology on mode I fracture toughness of cellular structures. Phys Mesomech 2018;21(2):178–86.
[35] Al-Fasih MY, Kueh ABH, Abo Sabah SH, Yahya MY. Influence of tows waviness and anisotropy on effective Mode I fracture toughness of triaxially woven fabric composites. Eng Fract Mech 2017;182:521–36.
[36] Srivastava VK, Gries T, Veit D, et al. Effect of nanomaterial on mode I and mode II interlaminar fracture toughness of woven carbon fabric reinforced polymer composites. Eng Fract Mech 2017;180:73–86.
[37] Marsavina L, Constantinescu DM, Linul E, et al. Evaluation of mixed mode fracture for PUR foams. Procedia Mater Sci 2014;3:1342–52.
[38] Arvidson JM, Sparks LL. Low temperature mechanical properties of a polyurethane foam. National Bureau of Standards, U.S. Department of Commerce, Colorado 80303, 1981.
[39] Farshidi A, Berggreen C, Carlsson LA. Low temperature mixed-mode debond fracture and fatigue characterisation of foam core sandwich. J Sandw Struct Mater 2018. https://doi.org/10.1177/1099636218779420.
[40] Demharter A. Polyurethane rigid foam, a proven thermal insulating material for applications between +130°C and −196°C. Cryogenics 1998;38:113–7.
[41] Yakushin VA, Zhmud NP, Stirna UK. Physicomechanical characteristics of spray-on rigid polyurethane foams at normal and low temperatures. Mech Compos Mater 2002;38(3):273–80.
[42] Stirna U, Beverte I, Yakushin V, Cabulis U. Mechanical properties of rigid polyurethane foams at room and cryogenic temperatures. J Cell Plast 2011;47(4):337–55.
[43] Denay AG, Castagnet S, Roy A, et al. Compression behavior of glass-fiber-reinforced and pure polyurethane foams at negative temperatures down to cryogenic ones. J Cell Plast 2013;49(3):209–22.
[44] Yakushin V, Cabulis U, Sevastyanova I. Effect of filler type on the properties of rigid polyurethane foams at a cryogenic temperature. Mech Compos Mater 2015;51(4):447–54.
[45] ASTM D5045. Standard test methods for plane-strain fracture toughness and strain energy release rate of plastic materials; 1999.
[46] EN ISO 179-2. Plastics – Determination of Charpy impact properties. Part 2: instrumented impact test; 2000.
[47] Kalthoff JF. Characterization of the dynamic failure behaviour of a glass-fiber/vinyl-seter at different temperatures by means of instrumented Charpy impact testing. Compos Part B-Eng 2004;35:657–63.
[48] Marsavina L, Linul E, Voiconi T, Sadowski T. A comparison between dynamic and static fracture toughness of polyurethane foams. Polym Test 2013;32:673–80.
[49] Marsavina L, Constantinescu DM, Linul E, et al. Refinements on fracture toughness of PUR foams. Eng Fract Mech 2014;129:54–66.
[50] ASTM D1622. Test method for apparent density of rigid cellular plastics; 2003.
[51] Movahedi N, Linul E, Marsavina L. The temperature effect on the compressive behavior of closed-cell aluminum-alloy foams. J Mater Eng Perform 2018;27(1):99–108.
[52] Linul E, Movahedi N, Marsavina L. On the lateral compressive behavior of empty and ex-situ aluminum foam-filled tubes at high temperature. Materials 2018;11(4):554.
[53] Yu YH, Choi I, Nam S, Lee DG. Cryogenic characteristics of chopped glass fiber reinforced polyurethane foam. Compos Struct 2014;107:476–81.
[54] Sperling LH. Introduction to physical polymer science. Wiley; 2006.
[55] Manson JA, Sperling LH. Polymer blends and composites. New York: Plenum; 1976.
[56] Mohammadi N, Yoo JN, Klein A, Sperling LH. A new instrument to study the role of chain rupture in the fracture of glassy polymer. J Polym Sci Polym Phys Ed 1992;30:1311.
[57] Linul E, Marşavina L, Linul PA, Kovacik J. Cryogenic and high temperature compressive properties of Metal Foam Matrix Composites. Compos Struct 2019;209:490–8.